Study of size effects in thin films by means of a crystal plasticity theory based on DiFT

Limkumnerd, S.; Van der Giessen, E.

Published in:
Journal of the Mechanics and Physics of Solids

DOI:
10.1016/j.jmps.2008.06.004

Publication date:
2008

Journal of the Mechanics and Physics of Solids 56 (2008) 3304–3314

Contents lists available at ScienceDirect

Journal of the Mechanics and Physics of Solids

journal homepage: www.elsevier.com/locate/jmps

Study of size effects in thin films by means of a crystal plasticity theory based on DiFT

S. Limkumnerd [a], E. Van der Giessen [b,*]

[a] Department of Physics, Faculty of Science, Chulalongkorn University, Phayathai Road, Patumwan, Bangkok 10330, Thailand
[b] Zernike Institute for Advanced Materials, University of Groningen, Nijenborgh 4, NL-9747 AG Groningen, The Netherlands

ARTICLE INFO

Article history:
Received 3 December 2007
Received in revised form
27 May 2008
Accepted 17 June 2008

Keywords:
Dislocations
Thin films
Size effects
Continuum plasticity
Dislocation correlations

ABSTRACT

In a recent publication, we derived the mesoscale continuum theory of plasticity for multiple-slip systems of parallel edge dislocations, motivated by the statistical-based nonlocal continuum crystal plasticity theory for single-glide given by Yefimov et al. [2004b. A comparison of a statistical-mechanics based plasticity model with discrete dislocation plasticity simulations. J. Mech. Phys. Solids 52, 279–300]. In this dislocation field theory (DiFT) the transport equations for both the total dislocation density and geometrically necessary dislocation (GND) density on each slip system were obtained from the Peach–Koehler interactions through both single and pair dislocation correlations. The effect of pair correlation interactions manifested itself in the form of a back stress in addition to the external shear and the self-consistent internal stress. We here present the study of size effects in single crystalline thin films with symmetric double slip using the novel continuum theory. Two boundary value problems are analyzed: (1) stress relaxation in thin films on substrates subject to thermal loading, and (2) simple shear in constrained films. In these problems, earlier discrete dislocation simulations had shown that size effects are born out of layers of dislocations developing near constrained interfaces. These boundary layers depend on slip orientations and applied loading but are insensitive to the film thickness. We investigate the stress response to changes in controlled parameters in both problems. Comparisons with previous discrete dislocation simulations are discussed.

1. Introduction

Contrary to the prediction of classical crystal plasticity theory, experimental observations at length scales ranging from hundreds of nanometers to tens of microns show size effects of the type "smaller is harder" (Ebeling and Ashby, 1966; Brown and Ham, 1971; Fleck et al., 1994; Ma and Clarke, 1995; Stölken and Evan, 1998; Arzt, 1998; McElhaney et al., 1998; Nix and Gao, 1998). This failure of conventional continuum theory is caused by the lack of a characteristic length scale. Several more sophisticated theories (Aifantis, 1984; Walgraef and Aifantis, 1985; Fleck and Hutchinson, 1993; Fleck et al., 1994; Gao et al., 1999; Huang et al., 2000, 2004; Ortiz and Repetto, 1999; Ortiz et al., 2000; Acharya and Bassani, 2000; Acharya and Beaudoin, 2000; Bassini et al., 2001; Gurtin, 2000, 2002, 2003) have been developed which, in various ways, include a length scale. Some of these theories attempt to incorporate this length scale through the concept of geometrically necessary dislocations (GNDs) as introduced by Nye (1953). In all theories, however, the length scale enters in an ad hoc

* Corresponding author. Tel.: +31 50 3638046; fax: +31 50 3634886.
E-mail addresses: surachate@sc.chula.ac.th (S. Limkumnerd), E.van.der.Giessen@rug.nl (E. Van der Giessen).

0022-5096/$ - see front matter © 2008 Elsevier Ltd. All rights reserved.
doi:10.1016/j.jmps.2008.06.004

fashion, and often has a constant value that needs to be supplied a priori by comparison with discrete dislocation simulations or experimental results.

Alternatively, Yefimov et al. (2004a, b) have applied a nonlocal continuum plasticity theory based on the works by Groma (1997) and Zaiser et al. (2001) to successfully solve a set of boundary value problems for systems with one active slip system.[1] They described the evolution of total dislocation densities and GND densities using a set of coupled transport equations. In addition to external shear and Peach–Koehler interactions among dislocations, the effect of pair–dislocation correlation, in the form of a back stress, was considered; the latter gave rise to a natural length scale $1/\sqrt{\rho}$, determined by the average dislocation density ρ. Thriving on the success of their theory, Yefimov and Van der Giessen (2005a, b) attempted to extend their single-slip theory to describe multiple-slip systems on phenomenological grounds. Albeit favorable results were obtained in the problem of shearing of thin films, the theory could not capture the size and orientation-dependent hardness observed in thin films.

To address this problem, we have reformulated the multiple-slip theory aiming to extract the correct angular dependence of the back stress between different pairs of slip orientations (Limkumnerd and Van der Giessen, 2008). By solving Bogolyubov–Born–Green–Yvon–Kirkwood (BBGYK) integral equations that relate different orders of dislocation correlation functions, the functional forms of pair–dislocation densities were derived. The results provided slip orientation dependence of pair densities from which the exact expression of the back stress was obtained. In their recent publication, Groma et al. (2006) arrived at the same expression for a pair correlation function in the case of single-slip systems.

We begin in Section 2 by giving a summary of our continuum theory with a short account to the work of Yefimov and Van der Giessen (2005a). In Section 3, we apply the theory to the problem of stress relaxation in single crystalline thin films on substrates subjected to thermal loading. It was this problem in which the results between the former multiple-slip theory (Yefimov and Van der Giessen, 2005b) and discrete dislocation simulations (Nicola et al., 2003, 2005b) deviated most. In a quasi-static limit, where dislocations rearrange themselves much faster than the stress increase in the film, an analytical solution is derived. The hardening effect due to the film thickness and comparisons with the discrete dislocation results can be directly investigated for two slip orientations. Finally in Section 4, we revisit the problem of the simple shear response of thin films, which was used by Yefimov and Van der Giessen (2005a) for selecting their slip-interaction law. Layers of dislocations form the top and bottom boundaries which give rise to size effects. Analytical solutions of our theory are checked against the discrete dislocation simulations by Shu et al. (2001).

2. Summary of DiFT based plasticity

Over a decade ago, Groma (1997) derived a set of transport equations governing the motion of many-dislocation densities by carrying out a statistical averaging procedure on ensembles of edge dislocations on parallel glide planes. Later on, Zaiser et al. (2001) specialized on these equations to describe evolution of single-dislocation densities in terms of pair–dislocation densities. Recently, the authors have extended the above formalism to include systems with more than one active slips (Limkumnerd and Van der Giessen, 2008). By constructing the integral equations that relate different orders of dislocation correlation functions, we explicitly calculate pair correlation functions, and hence pair–dislocation densities. In this section we shall briefly summarize this continuum theory, leaving the derivation to Limkumnerd and Van der Giessen (2008).

Consider a single crystal with N active slip systems where each system i is defined by slip direction $\mathbf{s}_i$ and slip plane normal $\mathbf{m}_i$. We assume that the motion of dislocations is overdamped; positive dislocations on slip system i flow with velocity $\mathbf{v}_i \equiv (\mathbf{b}_i/B)\,\tau_i^{\mathrm{eff}}$ in the direction of their Burgers vector $\mathbf{b}_i \equiv b\,\mathbf{s}_i$, with magnitude proportional to the effective resolved shear stress τ_i^{eff} with drag coefficient B, while negative dislocations flow in the opposite direction. The evolution equations for uncorrelated, single-dislocation densities ρ_i^+ and ρ_i^- can then be rewritten in terms of a set of coupled transport equations for total dislocation density $\rho_i \equiv \rho_i^+ + \rho_i^-$ and the GND density $\kappa_i \equiv \rho_i^+ - \rho_i^-$ as follows:

$$\partial_t \rho_i + \boldsymbol{\nabla}\cdot[\kappa_i \mathbf{v}_i] = 0, \quad \partial_t \kappa_i + \boldsymbol{\nabla}\cdot[\rho_i \mathbf{v}_i] = 0 \quad \text{(no sum over } i\text{)} \tag{1}$$

with $\boldsymbol{\nabla}$ the derivative with respect to spatial position $\mathbf{r}$. Nucleation and annihilation of dislocations can be taken into account by modifying the right-hand side of the evolution law for ρ_i (cf. Yefimov et al., 2004b). The dislocation density description can be incorporated into the framework of crystal plasticity through Orowan's relation

$$\dot{\gamma}_i = \frac{b^2}{B}\,\tau_i^{\mathrm{eff}}\rho_i \tag{2}$$

and the definition of plastic strain rate

$$\dot{\boldsymbol{\varepsilon}}^{\mathrm{p}} \equiv \sum_{i=1}^{N} \dot{\gamma}_i \boldsymbol{P}_i, \quad \boldsymbol{P}_i = \tfrac{1}{2}(\mathbf{s}_i \otimes \mathbf{m}_i + \mathbf{m}_i \otimes \mathbf{s}_i).$$

[1] Somewhat similar approaches have been taken by Arsenlis and Parks (2002), Arsenlis et al. (2004), El-Azab (2000), Limkumnerd and Sethna (2006), Acharya and Roy (2006), and Roy and Acharya (2006).

Substitution into the second dynamical equation (Eq. (1)) and time integration yields Kröner's relation

$$\kappa_i = -(1/b)(\mathbf{s}_i \cdot \boldsymbol{\nabla})\gamma_i, \tag{3}$$

which connects GND density κ_i to plastic slip γ_i.

The effective resolved shear stress

$$\tau_i^{\text{eff}} \equiv \tau_i - \tau_i^{\text{b}}, \tag{4}$$

consists of τ_i—the external shear stress plus the self-consistent, long-range, single-dislocation interaction—and the back stress τ_i^{b} given by

$$\tau_i^{\text{b}}(\mathbf{r}) = \frac{\mu b D}{2\pi(1-\nu)} \sum_{j=1}^{N} \cos(\theta_{ij}) \frac{(\mathbf{b}_j \cdot \boldsymbol{\nabla})\kappa_j(\mathbf{r})}{\rho_j(\mathbf{r})}, \tag{5}$$

arising from the short-range, dislocation–dislocation interactions. Here μ and ν are the shear modulus and the Poisson ratio, respectively. The strength of intra-slip back stress is controlled by the dimensionless constant D. The back stress contribution from slip system j to slip system i is reduced relative to the self back stress by a factor $\cos(\theta_{ij})$, where θ_{ij} is the angle between planes of slip system i relative to j.

The form of the back stress as shown in Eq. (5) reduces to that of the previous single-slip theory (Groma et al., 2003; Yefimov et al., 2004a, b) for $N = 1$. The $\cos(\theta_{ij})$ slip coupling should come as no surprise. The angular dependence of the back stress must reflect the symmetry of the Peach–Koehler interaction. The angular average of the interaction selects out $\cos(\theta_{ij})$ as the only possibility. The $\cos(\theta_{ij})$ coupling also appears in the strain-gradient theory for continuum crystal plasticity by Gurtin (2000, 2002, 2003). In an early attempt to extend their theory to describe systems with multiple slips, Yefimov and Van der Giessen (2005a) had considered three different coupling terms: $\cos^2(\theta_{ij})$, $\cos(2\theta_{ij})$, and $\cos(\theta_{ij})$. They subsequently discarded the first and the third variations upon comparisons with discrete dislocation simulations by Shu et al. (2001). Although the chosen form of coupling showed reasonable agreements with the discrete dislocation results in the problem of simple shearing of constrained thin film, it failed to capture the dependence on film size and slip orientation observed in the problem of stress relaxation in thin films on substrates (Yefimov and Van der Giessen, 2005b). We shall reexamine these problems with the new continuum theory in the following sections and argue that the success of the $\cos(2\theta_{ij})$-type coupling was just fortuitous.

3. Application to single crystal thin films on a substrate

In this section we consider the problem of stress relaxation in a single crystalline thin film, oriented for symmetric double-slip, on a substrate subjected to thermal loading. The geometry of the problem is shown in Fig. 1. Initially both the thin film, with thermal expansion coefficient α_f, and the substrate, with coefficient α_s, are at a (high) temperature T_0. Since $\alpha_f > \alpha_s$, a tensile stress up in the film as temperature decreases (with a rate $\dot{T}$). At sufficiently high stress, pairs of dislocations nucleate on the two active slips according to Frank–Read mechanism. When the material is assumed to be initially homogeneous, the problem is effectively one-dimensional; only variations along the direction perpendicular to the film matter and the only nonvanishing stress component is $\sigma_{xx} \equiv \sigma$. Also, by symmetry, $\gamma_1 = -\gamma_2$ and $\tau_1 = -\tau_2$. Hence, on average, the density of positive dislocations on the first slip is the same as that of negative dislocations on the second, while the negative of the first slip and the positive of the second are driven out of the system through the top traction-free surface. We shall henceforth drop the subscripts and only consider slip system 1.

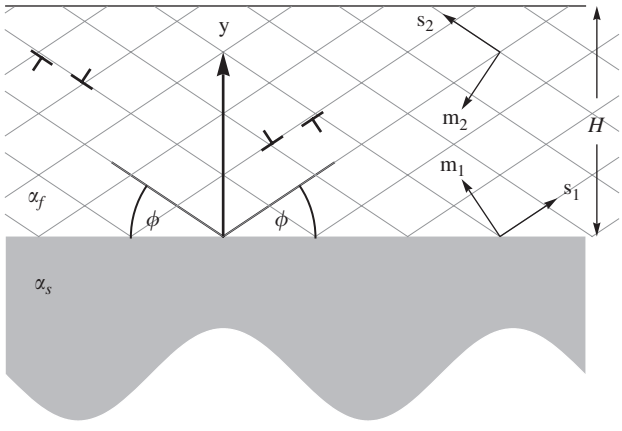

Fig. 1. A thin film of thickness H and thermal expansion coefficient α_f is situated on top of an infinite substrate with coefficient α_s. The film has two symmetrical slip planes defined by angle ϕ. The **y**-axis is taken to be perpendicular to the film–substrate interface.

This problem can be treated rather simply in a quasi-static limit where dislocations rearrange themselves much faster than the stress change. In this limit, the exact expressions for the nucleation and/or annihilation terms are unimportant and the nature of the evolution equation (1) is only to transport dislocations inside the thin film according to its overall effective stress. At any particular time, the distribution of these densities can be calculated from the competition between the back stress and the stress due to the thermal mismatch. Given the form of the back stress (5), we can derive the time dependence of this expression from the compatibility requirement in terms of slip γ_i on system 1 and 2. Using Kröner's relation (3), the time evolution of the overall resolved shear stress as a function of slip orientation can then be found. The effects of film thickness and slip orientation on the stress response can be investigated from these expressions.

In the absence of plasticity, the stress inside the film would build up according to

$$\sigma_{\mathrm{N}}(T) = 2\mu\left(\frac{1+\nu}{1-\nu}\right)\alpha(T_0 - T), \tag{6}$$

where $\alpha \equiv \alpha_{\mathrm{f}} - \alpha_{\mathrm{s}}$ is the effective expansion coefficient of the film relative to the substrate. Once the yield point is reached, $\sigma_{\mathrm{Y}} \equiv \sigma_{\mathrm{N}}(T_{\mathrm{Y}})$, plastic straining,

$$\dot{\varepsilon}_{xx} = -\dot{\gamma}\sin(2\phi),$$

is governed by the resolved shear stress

$$\tau = -\frac{\sin(2\phi)}{2}\sigma.$$

Compatibility of the thermally induced strain and the elastoplastic strains requires that after the yield point is reached,

$$(1+\nu)\alpha\,\Delta T = \frac{1-\nu}{2\mu}(\sigma - \sigma_{\mathrm{Y}}) - \gamma\sin(2\phi), \tag{7}$$

where $\Delta T \equiv T_{\mathrm{Y}} - T$ is the temperature drop since yield, and γ is the plastic slip (taken to be of slip system 1). The effective shear stress τ^{eff} comprises the resolved shear stress

$$\tau = -\frac{\sin(2\phi)}{2}\left[\sigma_{\mathrm{N}} + \frac{2\mu}{1-\nu}\gamma\sin(2\phi)\right], \tag{8}$$

and the back stress which, according to Eq. (5), is given by

$$\begin{aligned}\tau^{\mathrm{b}} &= \frac{\mu bD}{2\pi(1-\nu)\rho}\sin(\phi)\left[1-\cos(2\phi)\right]\partial_y\kappa \\ &= \frac{\mu bD\sin^3(\phi)}{\pi(1-\nu)\kappa}\,\partial_y\kappa,\end{aligned} \tag{9}$$

since $\rho = \kappa$ in this system. Combining Eqs. (7)–(9) with $\kappa = -\sin(\phi)/b\partial_y\gamma$ from Eq. (3), we can write the effective shear stress as

$$\tau^{\mathrm{eff}} = -\frac{\sin(2\phi)}{2}\frac{2\mu}{1-\nu}\left[\frac{1-\nu}{2\mu}\sigma_{\mathrm{N}} + \gamma\sin(2\phi) + \frac{bD}{\pi}\frac{\sin^3(\phi)}{\sin(2\phi)}\frac{\partial_y^2\gamma}{\partial_y\gamma}\right] \tag{10}$$

Under the quasi-static assumption mentioned above, the equation of motion (1) is solved by force balancing—in other words—by setting $\tau^{\mathrm{eff}} = 0$. Eq. (10) then gives the nonlinear differential equation

$$\frac{\zeta f(\phi)}{2}\partial_y^2\gamma + \partial_y\gamma\left[\gamma\sin(2\phi) + \frac{1-\nu}{2\mu}\sigma_{\mathrm{N}}\right] = 0 \tag{11}$$

with the length scale $\zeta \equiv 2bD/\pi$ being considered the new fitting parameter (instead of D). The solution during yield, subject to the no-slip condition $\gamma = 0$ at the film–substrate interface $y = 0$, is unique and given by

$$\sin(2\phi)\,\gamma = -\frac{1-\nu}{2\mu}\left[\sigma_{\mathrm{N}} - \sigma_{\mathrm{Y}}\frac{\sigma_{\mathrm{N}}\cosh(\lambda y) + \sigma_{\mathrm{Y}}\sinh(\lambda y)}{\sigma_{\mathrm{Y}}\cosh(\lambda y) + \sigma_{\mathrm{N}}\sinh(\lambda y)}\right], \tag{12a}$$

$$\lambda \equiv \frac{\varepsilon_{\mathrm{Y}}}{f(\phi)}\frac{1}{\zeta}. \tag{12b}$$

Here, $\varepsilon_{\mathrm{Y}} = (1+\nu)\alpha(T_0 - T_{\mathrm{Y}})$ is the film's strain at yield, and $f(\phi) \equiv \sin^3(\phi)/\sin(2\phi)$ contains the angular dependence on slip orientation. The stress profile after yield can be derived using Eq. (8):

$$\sigma(y,T) = \sigma_{\mathrm{Y}}\frac{\sigma_{\mathrm{N}}\cosh(\lambda y) + \sigma_{\mathrm{Y}}\sinh(\lambda y)}{\sigma_{\mathrm{Y}}\cosh(\lambda y) + \sigma_{\mathrm{N}}\sinh(\lambda y)} \tag{13}$$

The average stress over the thickness of the film, $\langle\sigma_{xx}\rangle \equiv (1/H)\int_0^H \sigma\,\mathrm{d}y$, follows directly from Eq. (13) as

$$\langle\sigma_{xx}(T)\rangle = \frac{\sigma_{\mathrm{Y}}}{\lambda H}\log\left[\cosh(\lambda H) + \frac{\sigma_{\mathrm{N}}(T)}{\sigma_{\mathrm{Y}}}\sinh(\lambda H)\right] \tag{14}$$

To compare results between the nonlocal theory and discrete dislocation simulations by Nicola et al. (2003) we use parameters from their simulation. The film is taken to be isotropic with Poisson's ratio $\nu = 0.33$, Young modulus $E = 70\,\text{GPa}$ (from which the value of $\mu = E/(2(1+\nu))$ is computed), and thermal expansion coefficient $\alpha_f = 23.2 \times 10^{-6}\,\text{K}^{-1}$. These values are representative of aluminum. The silicon substrate has expansion coefficient $\alpha_s = 4.2 \times 10^{-6}\,\text{K}^{-1}$. The system is cooled from an initial temperature of $T_0 = 600\,\text{K}$ down to $T = 400\,\text{K}$, at a rate of $\dot{T} = 4 \times 10^7\,\text{K/s}$. For the source density and source strength (distribution) chosen by Nicola et al. (2003), yield starts when the temperature reaches $T_Y \simeq 582\,\text{K}$, i.e. at $\sigma_Y \simeq 35.8\,\text{MPa}$.

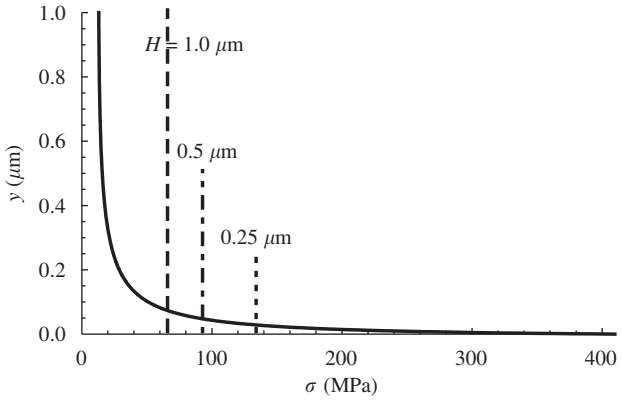

Fig. 2. Stress distribution across the film as predicted by Eq. (13) for $\phi = 60^\circ$. Vertical lines indicate the average stress in the films at different film thicknesses H.

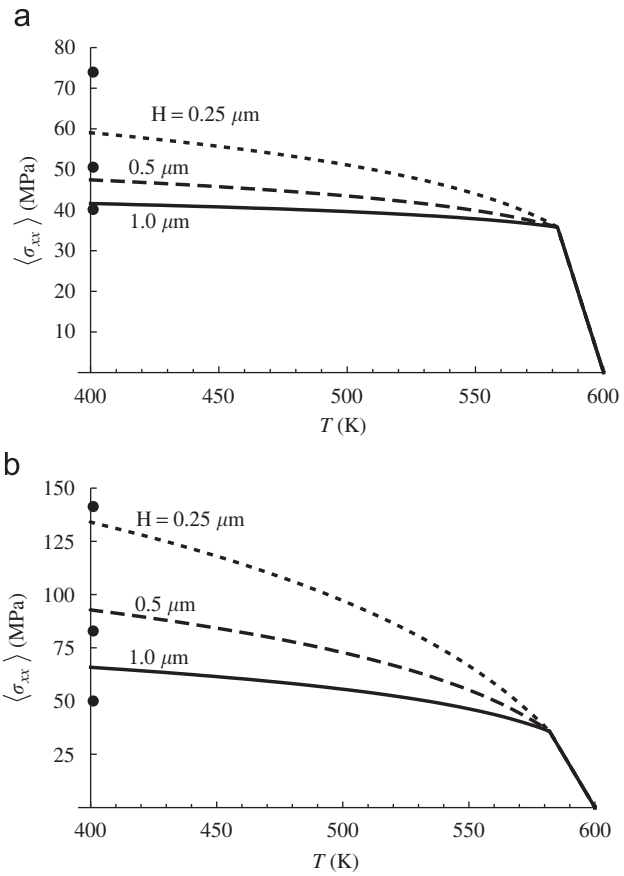

Fig. 3. Temperature dependence of average tensile stress $\langle\sigma_{xx}\rangle$ from Eq. (14) for slip orientations (a) $\phi = 30^\circ$ and (b) $\phi = 60^\circ$. The solid dots represent the discrete simulation results (Nicola et al., 2003).

Fitting to the average film stress at $T = 400\,\mathrm{K}$ predicted by the discrete dislocation simulations for orientation $\phi = 60^\circ$ yields a value of $\zeta \simeq 28.5\,\mathrm{nm}$. Fig. 2 shows the corresponding stress distribution across the film thickness according to Eq. (13). At the film–substrate interface, the stress σ reaches its elastic value of $\sigma_\mathrm{N} \simeq 397\,\mathrm{MPa}$, and decays roughly exponentially to the yield stress $\sigma_\mathrm{Y} \simeq 35.8\,\mathrm{MPa}$ at the free surface. This profile is independent of the film thickness H, as is the discrete dislocation result for the thickest two films. The average stress $\langle\sigma_{xx}\rangle$ for each thickness is indicated by a vertical line. The result for $\phi = 30^\circ$ exhibits a similar functional dependence but with a steeper decay, and is omitted for brevity.

Figs. 3(a) and (b) show the average stress $\langle\sigma_{xx}\rangle$ as a function of temperature T for different film thicknesses for $\phi = 30^\circ$ and 60°, respectively. When the temperature axis is read right-to-left as a measure of strain, these stress–strain curves are steeper (*film is harder*) as the thickness decreases. The hardening rate also increases with increasing ϕ, even though the Schmid factors for both orientations are identical. Finally, the prediction of the average tensile stress versus film thickness according to Eq. (14) is shown in Fig. 4 against the discrete dislocation results (in symbols) for both slip orientations with satisfactory agreement.

The thickness dependence of stress predicted by Eq. (14) is clearly a more complicated one than a simple scaling of the type $\langle\sigma_{xx}\rangle \propto H^{-p}$, with p varying usually between $1/2$ and 1. In order to see how large this deviation is, Fig. 5 shows the data of Fig. 4 on double-log scales. For $\phi = 60^\circ$, the theoretical $\langle\sigma_{xx}\rangle(H)$ is rather close to a power law over the entire regime considered here, but curves upwards for very small H when $\phi = 30^\circ$. Enhanced hardening in very thin films is observed in discrete dislocation results (Nicola et al., 2003, 2005b) and has been attributed there to dislocation sources being shut down by relatively long pile-ups; this effect is absent in the quasi-static solution developed here since nucleation is not taken into account. It is noted that a variability in the thickness scaling exponent is not only found in theoretical and numerical considerations but also in experiments, e.g. (Arzt, 1998; Venkatraman and Bravman, 1992; Baker et al., 2001; Yu and Spaepen, 2004). However, in the latter this is partly due to variations in experimental conditions: most experiments are carried out on polycrystalline films instead of single crystal films, as assumed here, and not all substrate materials can be expected to serve as perfect barriers to dislocation motion, as assumed here too. In polycrystalline films, the film thickness

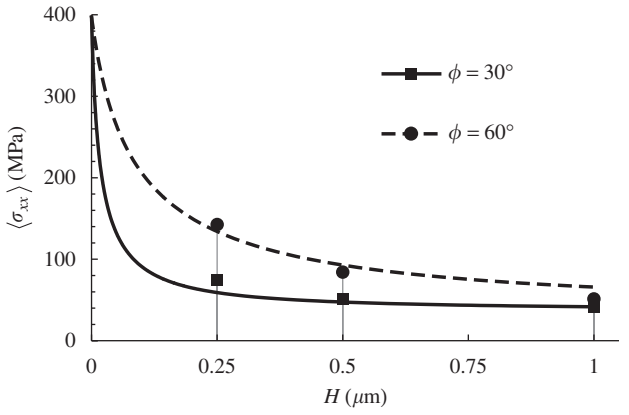

Fig. 4. Average stress at final temperature as a function of film thickness H for $\phi = 30^\circ$ and 60°. The symbols represent results from the discrete dislocation simulations.

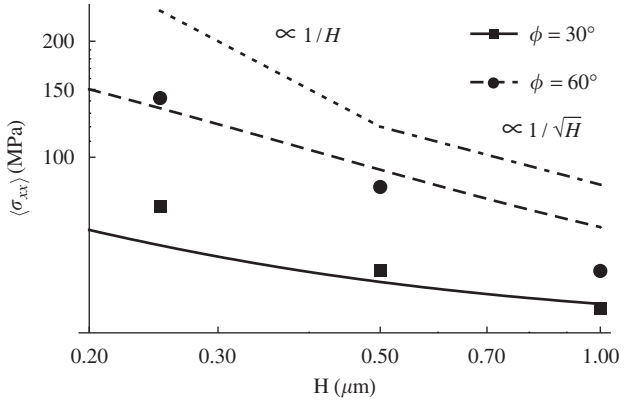

Fig. 5. Log–log plot of the same data as in Fig. 4, and comparison with simple power law scaling laws with exponents −0.5 and −1.

effect is coupled to the influence of grain size, and it is generally difficult experimentally to ascertain the relative roles of grain size and film thickness. Yet, quite commonly, the experimental value of the scaling exponent also varies between -0.5 and -1.

A similar theoretical study has been carried out by Nicola et al. (2005a) using Gurtin's strain-gradient theory. Compared to the discrete dislocation results, size-dependent hardening was captured but not the orientation dependence since Gurtin's original theory predicts the same response for $\phi = 30^\circ$ as for $\phi = 60^\circ$. Subsequently, they proposed a modified "defect energy" based on the consideration of dislocation pile-ups which did predict the correct ϕ-trend. The latter implies a material length scale that scales with $\cos\phi$, while our theory predicts scaling with $1/f(\phi) \propto \sin^2\phi/\cos\phi$; the ratio of these for $\phi = 30^\circ$ and 60° is identical. It is also interesting to note that the theory by Nicola et al. (2005a) reveals a constant hardening rate for a given thickness and slip orientation, whereas we find a weak logarithmic dependence on temperature. Both outcomes are within the error bar of the discrete dislocation results.

4. Simple shear of constrained film

We consider the same film as in the previous section, but now subjected to a shear Γ in the **x** direction, see Fig. 6. While the normal strain was uniform in the film under thermal straining, in the present problem the only nonvanishing stress component σ_{xy} is uniform across the width. The second difference is that now both surfaces are impenetrable for dislocations; i.e. $\gamma_1 = \gamma_2 = 0$ at $y = \pm H/2$ (note that the origin has been placed at the center of the film for calculational convenience). By symmetry, $\tau_1 = \tau_2$ and $\gamma_1 = \gamma_2$ which implies that $\kappa_1 = \kappa_2$ and $\rho_1 = \rho_2$. We shall therefore omit the subscripts.

We can again solve this problem quasi-statically in the manner of Section 3. The resolved shear stress τ_1 is given by

$$\tau = \cos(2\phi)\,\sigma_{xy}, \tag{15}$$

while the back stress τ^{b} is, according to Eq. (5),

$$\tau^{\mathrm{b}} = GDf(\phi)\,\frac{\partial_y\kappa}{\rho}, \tag{16}$$

where $G \equiv \mu b/(2\pi(1-\nu))$ contains all the material parameters, and $f(\phi) \equiv \sin(\phi)(1-\cos(2\phi)) = 2\sin^3(\phi)$ captures the slip orientation information. Force balancing, $\tau - \tau^{\mathrm{b}} = 0$, implies that

$$\sigma_{xy} = GD\,\frac{f(\phi)}{\cos(2\phi)}\,\frac{\partial_y\kappa}{\rho}. \tag{17}$$

Since σ_{xy} is uniform across the film thickness by virtue of equilibrium, we arrive at the differential equation

$$A(\phi)\partial_y\kappa(y) = \sigma_{xy}\rho(y), \tag{18}$$

above yield. Here $A(\phi) \equiv 2GD\sin^3(\phi)/\cos(2\phi)$ contains the slip orientation dependence.

Under shear, dislocations of one sign (negative when $\phi > \pi/4$) move towards the top $y = H/2$ where they are blocked, while the opposite-signed dislocations will pile-up against the bottom surface; this implies that $\kappa(y) = -\mathrm{sgn}(y)\rho(y)$. The solution of Eq. (18) is thus very simple:

$$\kappa(y) = -\mathrm{sgn}(y)\kappa_0\,\exp[\sigma_{xy}|y/A(\phi)|] \tag{19}$$

The constant of integration κ_0 in general could be a function of the applied shear Γ. Using the relationship (3) between GND density and slip, Eq. (19) together with the no-slip boundary conditions give

$$\gamma(y) = -\gamma_0(\Gamma)\{1 - \exp[\lambda(|y| - H/2)]\}, \tag{20}$$

where all the integration constants have been absorbed into $\gamma_0(\Gamma)$, and $1/\lambda \equiv |A(\phi)|/\sigma_{xy}(\Gamma)$ gives the approximate characteristic width of the boundary layers as a function of the applied shear Γ.

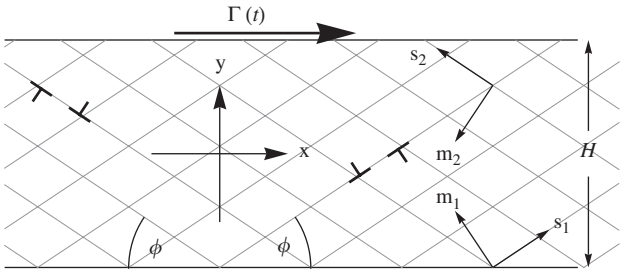

Fig. 6. The thin film of thickness H with two impenetrable top and bottom layers is under prescribed shearing $\Gamma(t)$. The film has two symmetrical slip planes defined by angle ϕ. The origin of the coordinate system is located at the center of the film.

Averaging of the decomposition $\varepsilon_{ij} = \varepsilon_{ij}^{\mathrm{E}} + \varepsilon_{ij}^{\mathrm{P}}$ across the width of the sample, along with Hooke's law $\sigma_{xy} = 2\mu\varepsilon_{xy}^{\mathrm{E}}$ gives

$$\sigma_{xy} = 2\mu(\Gamma/2 - \cos(2\phi)\langle\gamma\rangle). \tag{21}$$

Here, we have made use of the fact that $\langle\varepsilon_{xy}\rangle = \Gamma/2$ and employed Eq. (2) to find $\varepsilon_{xy}^{\mathrm{P}} = \cos(2\phi)\gamma$. The average slip can be calculated directly from Eq. (20),

$$\langle\gamma\rangle = -\gamma_0(\Gamma)\left[1 - \frac{1 - \mathrm{e}^{-\lambda H/2}}{\lambda H/2}\right]. \tag{22}$$

The functional form of $\gamma_0(\Gamma)$ can be obtained in the limit of large film thickness, $H \to \infty$, where the system is insensitive to the boundary layers which results in perfect plasticity. In this case Eq. (21) implies that

$$\tau_{\mathrm{Y}} = \mu\big(\Gamma + 2\cos(2\phi)\gamma_0\big). \tag{23}$$

Eqs. (21)–(23) together provide an implicit expression of σ_{xy} as a function of the applied shear Γ:

$$\sigma_{xy} = \tau_{\mathrm{Y}} + (\mu\Gamma - \tau_{\mathrm{Y}})\,\frac{1 - \mathrm{e}^{-\lambda H/2}}{\lambda H/2} \tag{24}$$

The continuum theory is tested against the discrete dislocation simulations by Shu et al. (2001) on a crystal with two slip systems oriented at $\phi = 60^\circ$. The elastic properties are the same as in Section 2, i.e. $\mu = 26.3$ GPa and $\nu = 0.33$, and stress is measured in units of the mean nucleation strength $\sigma_0 = 1.9 \times 10^{-3}\,\mu$ in the discrete simulations. We first note that the width of the boundary layers $1/\lambda$ cannot be used as a fitting parameter since its value changes with increasing stress. We therefore define the length parameter $l \equiv \sigma_{xy}/(\sigma_0\lambda) = |A|/\sigma_0$, which is independent of σ_{xy}, as a new fitting parameter. Given stress σ_{xy} at a selected shear Γ, the value of l can be determined from fitting Eq. (20) to the strain distribution across the film thickness, as shown in Fig. 7. The fitting procedure is somewhat intricate due to the nonalgebraic nature of Eq. (24) which needs to be computed for $\gamma(y)$ in Eq. (20) at a given Γ. We therefore take the stress value from the simulation stress–shear curve (Fig. 8) as an additional input for the fitting of l, yielding $l \simeq 46$ nm for the case of $H = 1\,\mu$m on the basis

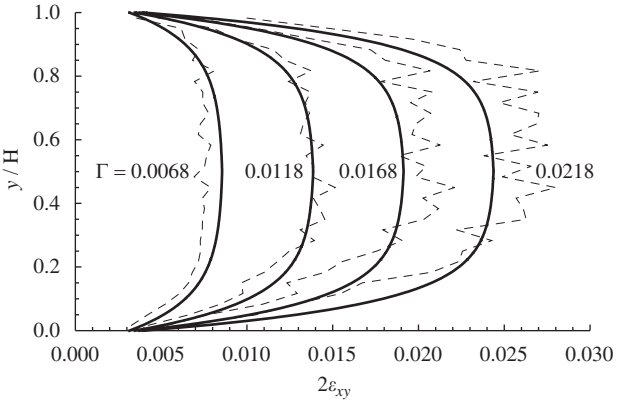

Fig. 7. Comparison of the discrete dislocation (Shu et al., 2001) (dashed lines) and nonlocal plasticity (solid curves) shear strain profiles at different values of the applied shear Γ for film thickness $H = 1\,\mu$m.

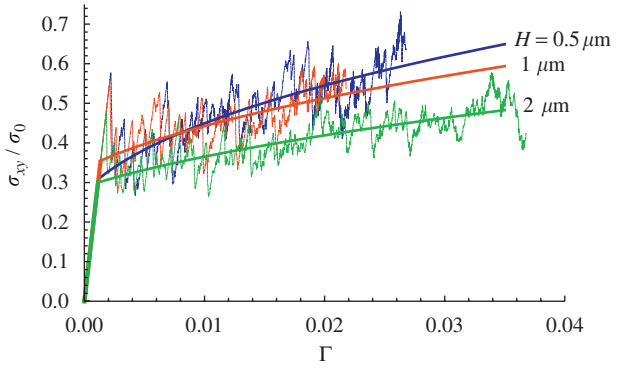

Fig. 8. Shear stress response to applied shear Γ for various film thicknesses. The discrete dislocation data (dashed lines) is taken from Shu et al. (2001).

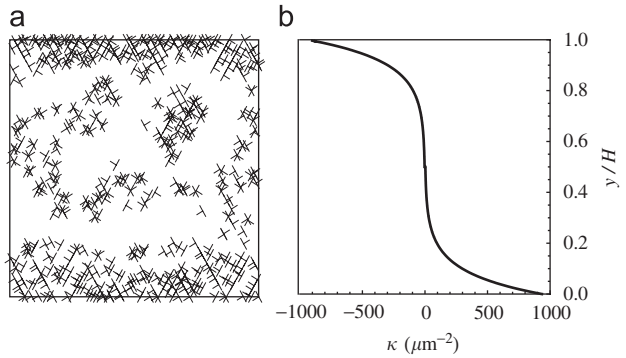

Fig. 9. Dislocation distribution in a $H = 1\,\mu$m thick $\phi = 60^\circ$ film at an overall shear of $\Gamma = 0.0218$ according to (a) discrete simulations by Shu et al. (2001) and (b) the theoretical solution (19) with $l \simeq 46$ nm.

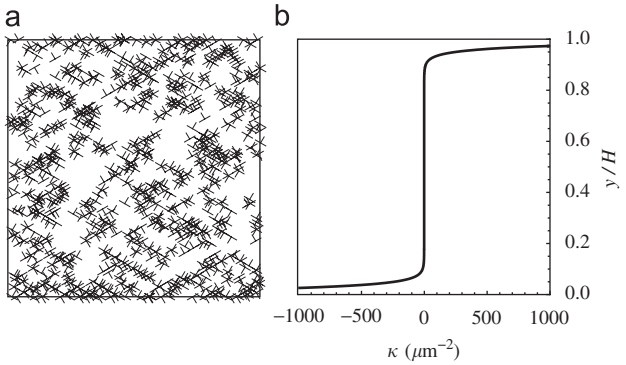

Fig. 10. Dislocation distribution in a $H = 1\,\mu$m thick $\phi = 30^\circ$ film at an overall shear of $\Gamma = 0.0218$ according to (a) discrete simulations by Shu et al. (2001) and (b) the theoretical solution (19) with $l \simeq 8.7$ nm.

of the stress at $\Gamma = 0.0218$. Fig. 7 shows shear strain distributions across the film thickness at three other values of Γ where no additional fitting has been performed.

For further comparison, Fig. 9(b) shows the theoretical distribution of dislocation density (recall that $\rho = \kappa$ for all slip systems) in comparison with the discrete dislocation distribution in a periodic cell with a width of $1\,\mu$m. The theory correctly predicts the development of intense dislocation boundary layers. The core of the crystal is left almost dislocation free as dislocations pass each other almost unhindered on their way towards the top and bottom faces.

From the above-mentioned best-fit l for the film thickness of $H = 1\,\mu$m, we can study the shear response for different film thicknesses. Data of the discrete dislocation simulations suggest thickness-dependent initial yield strengths. The responses are shown in Fig. 8 in comparison with results from the discrete simulations. We supply for each film thickness the best-fit yield point as an extra degree of freedom. Similar to the previous test problem (Section 3), the stress–strain curves show size-dependent hardening. The hardening rate decreases with increasing applied external shear, and approaches a constant value at large shear. Shu et al. (2001) also analyzed this problem with their version of strain-gradient theory and found weak size effects. Their stress response, however, is linear due to the fact that the width of dislocation boundary layers is constant in their theory. The same linear stress–strain relation was also predicted by Gurtin's strain-gradient theory (Bittencourt et al., 2003).

It should be mentioned that the exact form of the slip–interaction coupling (in Eq. (5)) turns out to be unimportant in this problem. The slip orientation dependence is buried inside the definition of $|A(\phi)|$ which has been absorbed into the fitting parameter l. On this ground, it does not matter whether this coupling be $\cos(\theta_{ij})$ or $\cos(2\theta_{ij})$ as proposed by Yefimov and Van der Giessen (2005a).

Our theory predicts drastic changes in behavior when ϕ crosses 45°. Due to a sign change in the resolved shear stress, the charges of dislocations at the two interfaces reverse from the present situation when $\phi < 45^\circ$ (resulting in the sign alternations of κ_0 and γ_0 in Eqs. (19), (20), (22), and (23)). As a result, the applied shear acts in favor of the new dislocation arrangement—in other words—our theory predicts that the back stress further enhances plasticity instead of impeding the flow of new dislocations into the boundaries. Hence, thinner boundary layers are expected which suggests smaller size effects. More quantitatively, for the orientation angle of, say, $\phi = 30^\circ$, the layers should be thinner by a factor of $l_{30^\circ}/l_{60^\circ} = |A(30^\circ)/A(60^\circ)| = (\sin(30^\circ)/\sin(60^\circ))^3 \simeq 0.19$. The dislocation distribution thus predicted is shown in Fig. 10(b).

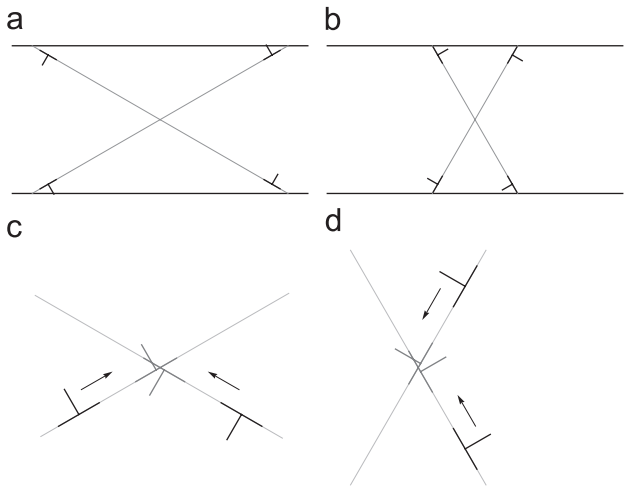

Fig. 11. Types of dislocations at the pile-ups for (a) $\phi = 30^\circ$ and (b) $\phi = 60^\circ$, and their locking situations as they glide (a) upwards or downwards (as viewed upside down) for 30° case or (d) in the opposite directions for 60° case.

Discrete dislocation dynamics simulations, however, reveal essentially no boundary layers at all—or, equivalently, boundary layers that span the entire width (Fig. 10(a)). Upon closer examination, we find 'locks' of dislocations[2] of like charges on different slip systems which prevent their motion pile-ups to the boundaries. A pair of dislocations with the relative angle of their Burgers vectors between 90° and 270° feel their mutual attraction when they glide past each other. Although rather weak, this interaction is apparently strong enough in this case for locking to occur. Figs. 11(a) and (b) show the types of dislocations which accumulate at the boundaries for $\phi = 30^\circ$ and 60°, respectively. Figs. 11(c) and (d) demonstrate one of the two situations when locking happens in each case (the others are 180° rotations of these). In the region sufficiently far away from the boundaries, event shown in Fig. 11(c) is roughly as likely to occur as event shown in Fig. 11(d), since the situations differ just by a 90° rotation followed by a flip about the **y**-axis. The relative likelihood, however, increases immensely close to the boundaries because only in the 30° case do dislocations moving to the same boundary permit locking, Fig. 11(c). This mutual locking of slip systems prevents dislocations to reach the boundaries and form localized boundary layers. The locking mechanism is purely a discrete phenomena and cannot be captured by the current continuum theory without further refinement. Due to its relatively small probability, locking seldom occurs in the 60° case.

5. Discussion and conclusion

We applied the recently formulated multiple-slip continuum plasticity theory to analyze two boundary value problems relating to thin films. In Section 3, we studied stress relaxation mechanism in thin films on substrates with thermal loading. We obtained an explicit analytical expression of the stress distribution as a function of slip orientation with one fitting parameter. The predictions were in good agreement with the discrete dislocation results of Nicola et al. (2003, 2005b). Our theory was able to show size-dependent hardening and the hardening due to slip orientations—both of which the previous continuum theory failed to explain. Subsequently, we analyzed simple shear in constrained films. Similarly to the first problem, we observed dislocation pile-ups at the top and bottom constrained boundaries. The thickness of dislocation layers depends weakly on the incremental shear. Regardless of the difference between the forms of slip–interaction coupling between our theory and that in Yefimov and Van der Giessen (2005a), our theory also gave satisfactory agreements with results from discrete dislocation dynamics simulations (Shu et al., 2001). We pointed out that this term can be absorbed into fitting parameter; the correct functional form of the coupling, therefore, cannot be decided only on the basis of this problem.

Acknowledgment

We acknowledge funding from the European Commissions Human Potential Programme SizeDepEn under contract number MRTN-CT-2003-504634.

[2] The use of the phrase 'locks' for parallel edge dislocations is somewhat inappropriate, because such dislocations only interact through their long-range field but do not alter the topology as happens in, e.g. Lomer locks. We nevertheless use the term here because it expresses the small-scale interactions that obstruct dislocation motion.

References

Acharya, A., Bassani, J.L., 2000. Incompatibility and crystal plasticity. J. Mech. Phys. Solids 48, 1565–1595.

Acharya, A., Beaudoin, A.J., 2000. Grain-size effect in viscoplastic polycrystals at moderate strains. J. Mech. Phys. Solids 48, 2213–2230.

Acharya, A., Roy, A., 2006. Size effects and idealized dislocation microstructure at small scales: predictions of a phenomenological model of mesoscopic field dislocation mechanics: part I. J. Mech. Phys. Solids 54, 1687–1710.

Aifantis, E.C., 1984. Towards a continuum approach to dislocation patterning. In: Markenscoff, X. (Ed.), Dislocations in Solids—Recent Advances, AMD-63. ASME, pp. 23–33.

Arsenlis, A., Parks, D.M., 2002. Modeling the evolution of crystallographic dislocation density in crystal plasticity. J. Mech. Phys. Solids 50, 1979–2009.

Arsenlis, A., Parks, D.M., Becker, R., Bulatov, V.V., 2004. On the evolution of crystallographic dislocation density in non-homogeneously deforming crystals. J. Mech. Phys. Solids 52, 1213–1246.

Arzt, E., 1998. Size effects in materials due to microstructural and dimensional constraints: a comparative review. Acta Mater. 16, 5611–5626.

Baker, S.P., Kretschmann, A., Arzt, E., 2001. Thermomechanical behavior of different texture components in cu thin films. Acta Mater. 49, 2145–2160.

Bassini, J.L., Needleman, A., Van der Giessen, E., 2001. Plastic flow in a composite: a comparison of nonlocal continuum and discrete dislocation predictions. Int. J. Solids Struct. 38, 833–853.

Bittencourt, E., Needleman, A., Gurtin, M.E., Van der Giessen, E., 2003. A comparison of nonlocal continuum and discrete dislocation plasticity predictions. J. Mech. Phys. Solids 51, 281–310.

Brown, L.M., Ham, R.K., 1971. Dislocation–particle interactions. In: Kelly, A., Nicholson, R.B. (Eds.), Strengthening Methods in Crystals. Elsevier, Amsterdam, pp. 12–135.

Ebeling, R., Ashby, M.F., 1966. Dispersion hardening of copper single crystals. Philos. Mag. 13, 805–834.

El-Azab, A., 2000. Statistical mechanics treatment of the evolution of dislocation distributions in single crystals. Phys. Rev. B 61 (18), 11956.

Fleck, N.A., Hutchinson, J.W., 1993. A phenomenological theory for strain gradient effects in plasticity. J. Mech. Phys. Solids 41, 1825–1857.

Fleck, N.A., Muller, G.M., Ashby, F., Hutchinson, J.W., 1994. Strain gradient plasticity: theory and experiment. Acta Metall. Mater. 42, 475–487.

Gao, H., Huang, Y., Nix, W.D., Hutchinson, J.W., 1999. Mechanism-based strain gradient plasticity I. Theory. J. Mech. Phys. Solids 47, 1239–1263.

Groma, I., 1997. Link between the microscopic and mesoscopic length-scale description of the collective behavior of dislocations. Phys. Rev. B 56 (10), 5807–5813.

Groma, I., Csikor, F.F., Zaiser, M., 2003. Spatial correlations and higher-order gradient terms in a continuum description of dislocation dynamics. Acta Mater. 51, 1271–1281.

Groma, I., Györgyi, G., Kocsis, B., 2006. Debye screening of dislocations. Phys. Rev. Lett. 96, 165503.

Gurtin, M.E., 2000. On the plasticity of single crystals: free energy, microforces, plastic-strain gradients. J. Mech. Phys. Solids 48, 898–1036.

Gurtin, M.E., 2002. A gradient theory of single-crystal viscoplasticity that accounts for geometrically necessary dislocations. J. Mech. Phys. Solids 50, 5–32.

Gurtin, M.E., 2003. On a framework for small-deformation viscoplasticity: free energy, microforces, strain gradients. Int. J. Plast. 19, 47–90.

Huang, Y., Gao, H., Nix, W.D., Hutchinson, J.W., 2000. Mechanism-based strain gradient plasticity II. analysis. J. Mech. Phys. Solids 48, 99–128.

Huang, Y., Qu, S., Hwang, K.C., Li, M., Gao, H., 2004. A conventional theory of mechanism-based strain gradient theory. Int. J. Plast. 20, 753–782.

Limkumnerd, S., Sethna, J.P., 2006. Mesoscale theory of grains and cells: crystal plasticity and coarsening. Phys. Rev. Lett. 96, 095503.

Limkumnerd, S., Van der Giessen, E., 2008. Statistical approach to dislocation dynamics: from dislocation correlations to formulation of multiple-slip continuum plasticity theory. Phys. Rev. B. 77, 184111.

Ma, Q., Clarke, D.R., 1995. Size dependent hardness of silver single crystals. J. Mater. Res. 10, 853–863.

McElhaney, K.W., Vlassak, J.J., Nix, W.D., 1998. Determination of indenter tip geometry and indentation contact area for depth-sensing indentation experiments. J. Mater. Res. 13 (5), 1300–1306.

Nicola, L., Van der Giessen, E., Needleman, A., 2003. Discrete dislocation analysis of size effects in thin films. J. Appl. Phys. 93, 5920–5928.

Nicola, L., Van der Giessen, E., Gurtin, M.E., 2005a. Effect of defect energy on strain-gradient predictions of confined single-crystal plasticity. J. Mech. Phys. Solids 53, 1280–1294.

Nicola, L., Van der Giessen, E., Needleman, A., 2005b. Two hardening mechanisms in single crystal thin films studied by discrete dislocation plasticity. Philos. Mag. 85, 1507–1518.

Nix, W.D., Gao, H., 1998. Indentation size effects in crystalline materials: a law for strain gradient plasticity. J. Mech. Phys. Solids 46 (3), 411–425.

Nye, J.F., 1953. Some geometrical relations in dislocated crystals. Acta Metall. 1, 153–162.

Ortiz, M., Repetto, E.A., 1999. Nonconvex energy minimization and dislocation structures in ductile single crystals. J. Mech. Phys. Solids 47, 397–462.

Ortiz, M., Repetto, E.A., Stainier, L., 2000. A theory of subgrain dislocation structures. J. Mech. Phys. Solids 48, 2077–2114.

Roy, A., Acharya, A., 2006. Size effects and idealized dislocation microstructure at small scales: predictions of a phenomenological model of mesoscopic field dislocation mechanics: part II. J. Mech. Phys. Solids 54, 1711–1743.

Shu, J.Y., Fleck, N.A., Van der Giessen, E., Needleman, A., 2001. Boundary layers in constrained plastic flow: comparison of nonlocal and discrete dislocation plasticity. J. Mech. Phys. Solids 49, 1361–1395.

Stölken, J.S., Evan, A.G., 1998. A microbend test method for measuring the plasticity length scale. Acta Mater. 46, 5109–5115.

Venkatraman, R., Bravman, J.C., 1992. Separation of film thickness and grain boundary strengthening effects in al thin films on si. J. Mater. Res. 7 (8), 2040–2048.

Walgraef, D., Aifantis, E.C., 1985. On the formation and stability of dislocation patterns -I, -II, -III. Int. J. Eng. Sci. 23, 1351–1372.

Yefimov, S., Groma, I., Van der Giessen, E., 2004a. Bending of a single crystal: discrete dislocation and nonlocal crystal plasticity simulations. Modell. Simulation Mater. Sci. Eng. 12, 1069–1086.

Yefimov, S., Groma, I., Van der Giessen, E., 2004b. A comparison of a statistical-mechanics based plasticity model with discrete dislocation plasticity simulations. J. Mech. Phys. Solids 52, 279–300.

Yefimov, S., Van der Giessen, E., 2005a. Multiple slip in a strain-gradient plasticity model motivated by a statistical-mechanics description of dislocations. Int. J. Solids Struct. 42, 3375–3394.

Yefimov, S., Van der Giessen, E., 2005b. Size effects in single crystal thin films: nonlocal crystal plasticity simulations. Eur. J. Mech. A—Solid 24, 183–193.

Yu, D.Y.W., Spaepen, F., 2004. The yield strength of thin copper films on kapton. J. Appl. Phys. 95 (6), 2991–2997.

Zaiser, M., Miguel, M.C., Groma, I., 2001. Statistical dynamics of dislocation systems: the influence of dislocation–dislocation correlations. Phys. Rev. B 64, 224102.